Quantitative Product Spectrum Analysis of Poly(butyl acrylate) via Electrospray Ionization Mass Spectrometry

Sandy P. S. Koo,[†,‡] Thomas Junkers,*[,†] and Christopher Barner-Kowollik*[,†]

Preparative Macromolecular Chemistry, Institut für Technische Chemie und Polymerchemie, Universität Karlsruhe (TH)/Karlsruhe Institute of Technology (KIT), Engesserstrasse 18, 76128 Karlsruhe, Germany, and Centre for Advanced Macromolecular Design (CAMD), School of Chemical Sciences and Engineering, The University of New South Wales, NSW 2052, Australia

Received May 30, 2008; Revised Manuscript Received October 13, 2008

ABSTRACT: Electrospray ionization mass spectrometry (ESI-MS) is used to analyze poly(butyl acrylate) samples at full conversion obtained by bulk free radical polymerization in the temperature range of 60−140 °C in the presence of the chain transfer agent (CTA) 1-octanethiol at concentrations varying between 0 and 0.4 mol·L^{-1}. Termination by combination products carrying initiator and transfer-derived fragments as well as three β-scission products were identified in the accessible mass range of up to 2000 *m*/*z*. The resulting mass spectra are subsequently quantitatively evaluated via integration to assess product distributions as a function of varying reaction conditions, that is, different temperatures and CTA concentrations. The present study provides for the first time quantitative product distribution data for butyl acrylate polymerization. The main species of interest, defined to be those most sensitive to variations in temperature, CTA concentration, or both, are identified to be thiol-capped polymers (TCPs) produced by the interference of the CTA in the polymerization and β^{I}, the β-scission product produced by chain cleavage of so-called midchain radicals formed via transfer to polymer reactions. Relatively high concentrations of 1-octanethiol produce a very uniform thiol-capped polymer, whereas low concentrations of thiol produce a very large number of β-scission products. Increasing the reaction temperature increases the proportions of β-scission products, and increasing the CTA concentration can suppress and control the amounts and types of species formed to the point where the product spectrum is almost quantitatively constituted of the TCP product. Other species found include conventional termination via combination products and small amounts of β-scission products with initiator end groups. The quantity of combination products has no significant variation under the range of conditions studied, and they are thus considered minor products. The data provided in the present study can constitute the basis for the further quantitative evaluation of reliable rate coefficients for midchain radical formation and depletion pathways.

Introduction

The mechanism of acrylate polymerization significantly differs from the ideal free radical polymerization (FRP) reaction scheme, which is reflected by the observation of reaction orders ω in monomer concentrations larger than unity (where $R_P \approx c_M{}^{\omega} c_R$, with R_P being the overall polymerization rate, c_M being the monomer concentration, and c_R being the radical concentration).[1] It is now widely accepted that these differences are due to the presence of so-called midchain radicals (MCRs).[2] Furthermore, it is recognized that this type of radical is responsible for the failure of low frequency pulsed laser polymerization size exclusion chromatography (PLP-SEC) experiments in the determination of the propagation rate coefficients at temperatures above room temperature.[3,4] MCRs are formed when the radical functionality of the secondary propagating radical (SPR) is transferred to the polymer backbone via chain transfer to polymer reactions through an H-shift reaction;[5−8] its products can be imaged using ESR spectroscopy.[9,10] Mechanistically, these reactions can proceed via intramolecular pathways, commonly referred to as backbiting, as well as via intermolecular reactions. In both cases a more stabilized tertiary radical is formed. Backbiting is favored to occur via a [1,5] H shift or to more remote positions. This MCR can subsequently undergo propagation, albeit at a significantly reduced rate; it may terminate with any other radical present in the system, or it may undergo β-scission reactions, forming unsaturated dead polymer and shortened propagating macroradicals.[6,11,12] Although not all individual reaction rate coefficients are available, an increasing number of data have become available in recent years, especially on the backbiting and MCR propagation reaction.[13,14]

The development of modern soft ionization mass spectrometry techniques such as matrix-assisted laser desorption ionization time-of-flight (MALDI-TOF) spectrometry and ESI-MS has provided a convenient means for unambiguously determining the product spectrum of a polymer sample and many changes within the chain length distribution.[15−18] This has created vast opportunities for in-depth polymer characterization at a level of detail that was previously unavailable. The potential of ESI-MS for exploring mechanistic aspects of radical polymerization has been discussed in a feature article,[15] and the impact of ESI-MS on the characterization of synthetic polymers has been reviewed.[19−25] Alternatively, NMR spectroscopy can also be used for acquiring information regarding end-group composition; however, this process can be time-consuming and can be hindered by the relative insensitivity and sometimes low solubility of branched polyacrylates. Furthermore, mass spectrometric analysis has an important advantage over NMR with respect to end-group composition in that MS is not dependent on the polymer chain length because each individual polymer chain appears in the spectrum, whereas in NMR, only an average overall present chain length is observed. Furthermore, NMR rapidly loses sensitivity with increasing DP_n because the end-group signal becomes weaker compared with the backbone signals. Hence, quantitative end-group information, especially at larger DP_n values, is associated with high experimental errors.

* Corresponding authors. Tel: +49 721 608-5641. Fax: +49 721 608-5740. E-mail: thomas.junkers@polymer.uni-karlsruhe.de; christopher.barner-kowollik@polymer.uni-karlsruhe.de.
† Universität Karlsruhe (TH)/Karlsruhe Institute of Technology (KIT).
‡ The University of New South Wales.

10.1021/ma801196w CCC: $40.75
Published on Web 11/25/2008

For example, if a polymer with an average chain length of 10 is analyzed and an error in the NMR signal of 5% is assumed (compared with the main peaks), then the end-group compositions are derived with higher absolute errors. In contrast, with mass spectrometry, the resulting uncertainty in end-group composition is directly given by the error of the signal intensity. Therefore, even if the primary experimental error might be higher in ESI-MS because of ionization effects, more accurate composition data for the single species can be derived from it.

Under certain circumstances, soft ionization techniques can be problematic in the analysis of polymers because they may not be fully quantitative when compounds of different ionization potential are analyzed. Additionally, they are restricted to lower molecular weight material. Yet, they allow product spectrum imaging in great detail and with high accuracy, and hence these techniques are able to provide information that cannot be obtained by other methods, such as the exact composition and distribution of the polymeric chains. Such knowledge is very advantageous when one contemplates the currently unresolved problems arising from MCR formation. To date, a range of studies employing ESI-MS to investigate the mechanism and kinetics of FRP, ranging from the analysis of RAFT polymers to photo- and thermal initiation systems, have been carried out. Most recently, Barner-Kowollik and coworkers studied photoinitiation processes in methacrylate, acrylate, and itaconate systems[16,17] as well as complex macromolecular architecture formation[26,27] via ESI-MS. Contemporarily, Buback and coworkers studied initiation pathways using peroxides.[28−30] Specific ESI-MS spectra for acrylate systems have recently been provided by us[31] and Simonsick and coworkers (for the distinct high-temperature polymerization of butyl acrylate (BA) in xylene solution).[32,33] Because soft ionization mass spectrometry allows for very detailed characterization and mapping of the reactions that take place during polymerization, it is a matter of priority to carry out a systematic MS study directed toward investigating the behavior and effects that MCR reactions have on overall product spectrum distributions in acrylate polymerizations. The ultimate goal of using this approach and the related quantitative information is to deduce kinetic information, that is, the β-scission, MCR termination, and backbiting rate pertaining to acrylate polymerizations that have proven difficult to arrive at thus far. In our last contribution, we gave a full assignment of all species present in a chain-transfer polymerization of BA.[31] The current study now aims to provide the quantitative analysis of such data under a broad range of experimental conditions. This product distribution data can subsequently find use in a kinetic modeling analysis. We note, however, that the limitations in the observable mass range from the ESI-MS technique need to be considered when such quantitative data are used for kinetic modeling. It cannot a priori be concluded that the accessible low molecular mass range is representative of the full molecular weight distribution, which may stretch up to 100 000 or millions of $g \cdot mol^{-1}$. For this reason, models need to be applied that allow for a specific output for a certain mass range. Such models can be constructed with relative ease via the program package PREDICI and can be used for data fitting, as we have demonstrated before.[34]

Concomitantly, we demonstrate that ESI-MS spectra can indeed be integrated in a quantitative fashion when the ionization potentials of all present species are similar. Such an approach can not only be applied to the present line of work but also has potential for quantitative analysis of other polymer product spectra and therefore represents an important advance for ESI-MS analysis in general.

Experimental Section

Materials. Butyl acrylate (BA, Fluka, 99%) monomer was deinhibited over a column of activated basic alumina. 2,2-Azoisobutyronitrile (AIBN) and 1,1-azobis(cyclohexanecarbonitrile) (ACHN, both DuPont) were both recrystallized twice from ethanol. 1-Octanethiol (Aldrich, 98.5%) was used as received. The solvents THF (Sigma-Aldrich, 99.9%, anhydrous, inhibitor-free) and methanol (MeOH) (Ajax, HPLC grade) were used as received.

Polymerization. All samples were prepared as follows: Each sample consisted of BA monomer (sample volume ~2.0 mL) with a photoinitiator concentration of 5×10^{-3} mol L^{-1} and a 1-octanethiol concentration of 0 to 0.4 mol L^{-1}. BA and photoinitiator were placed in a Schlenk flask and degassed according to the freeze−pump−thaw method. A Julabo HD-4 oil bath was used to perform the polymerization, allowing for a rapid temperature equilibration and hence heating-up periods that were as short as possible. AIBN was used for polymerizations at temperatures up to 100 °C, and ACHN was used for reaction temperatures above 100 °C. Samples were cooled in ice water to stop any further reaction once the required polymerization time was achieved, which was calculated by doubling the time estimated from the first-order kinetic decomposition equation to result in the full dissociation of the initiator into radicals (i.e, until >99% of initiator was decomposed). Monomer conversion was determined by gravimetry.

Electrospray Ionization Mass Spectrometry. ESI-MS experiments were carried out using a Thermo Finnigan LCQ Deca quadrupole ion-trap mass spectrometer (Thermo Finnigan, San Jose, CA) in positive ion mode. The ESI-MS was equipped with an atmospheric pressure ionization source that operated in nebulizer-assisted electrospray mode. The instrument was calibrated with caffeine, MRFA, and Ultramark 1621 (all from Aldrich) in the mass range of 195−1822 amu. All spectra were acquired over the mass-to-charge range (m/z) of 150−2000 Da with a spray voltage of 5 kV, a capillary voltage of 39 V, and a capillary temperature of 275 °C. Nitrogen was used as sheath gas (flow: 40% of maximum), whereas helium was used as auxiliary gas (flow: 5% of maximum in all experiments). The eluent was a 6:4 v/v mixture of THF/methanol with a polymer concentration of ~0.4 $mg \cdot mL^{-1}$. The instrumental resolution of the employed experimental setup was 0.1 Da. All reported theoretical molecular weights were calculated via the program package CS ChemDraw 6.0 and are monoisotopic.

Prior to making ESI-MS measurements, samples with a thiol concentration of <0.1 $mol \cdot L^{-1}$ were fractionated through the SEC setup in which samples of polymer concentrations of up to 150 $mg \cdot mol^{-1}$ were injected to obtain reasonably concentrated low-molecular-weight samples. The fraction corresponding to molecular weights between 2350 and 200 $g \cdot mol^{-1}$ was collected; it was subsequently mixed with methanol in a ratio of 3:2 and was directly subjected to ESI-MS analysis.

Size Exclusion Chromatography. Molecular weight distributions (MWDs) for the polymers were measured via SEC on a Shimadzu modular LC system comprising a ERC-3415 solvent degasser, a LC-10AT pump, a SIL-10AD autoinjector, a CTO-10A column oven, and a RID-10A refractive index detector. The system was equipped with a Phenomenex 5.0 μm bead-size guard column (50 × 7.5 mm), followed by four Phenomenex columns (106, 104, 103, and 500 Å). The eluent was THF at 40 °C with a flow rate of 1 $mL \cdot min^{-1}$. Calibration curves were generated using polystyrene standards in the molecular weight range of 580 to 1.95×10^6 $g \cdot mol^{-1}$. The injection volume was 50 μL (3−5 $mg \cdot mL^{-1}$). Molecular weights were obtained using the principle of universal calibration employing the Mark−Houwink−Kuhn−Sakurada (MHKS) constants of poly(butyl acrylate) ($K = 12.2 \times 10^{-3}$ $mL \cdot g^{-1}$ and $a = 0.70$)[35] and of polystyrene ($K = 14.1 \times 10^{-5}$ $mL \cdot g^{-1}$ and $a = 0.70$).[36]

Data Analysis

Conversion was determined gravimetrically, and all samples were found to have a conversion of ≥95%. Mass spectra were processed with Xcalibur, and an Excel spreadsheet was set up to integrate the mass spectra.

Integration. Integrations of all peaks of interest in the mass spectrum distribution were made using an appropriate spread-

sheet number analysis package by applying the principle of area calculation via the trapezoidal rule

$$\text{Area} = \int_a^b f\left(\frac{m}{z}\right) \mathrm{d}\frac{m}{z} \approx \Delta\frac{m}{z}\left(\frac{A_0}{2} + A_1 + A_2 + A_3 + ... + \frac{A_n}{2}\right) \quad (1)$$

whereby incremental areas formed under the peaks of the mass spectrum were calculated and summed over the relevant mass ranges to provide a measure of area. (See Figure S1 in the Supporting Information for definition of variables.) In this case, each relevant peak in the mass spectrum is individually calculated. The entire isotopic pattern of a species was integrated in the entire mass range, as opposed to each peak in the isotopic pattern being integrated individually and then summed for one species. This constitutes the integral of one peak in one repeat unit. The integral area of each species in each repeat unit was determined and subsequently summed to provide the total area of that species over the entire spectrum. This area is directly proportional to the concentration of the species because MS provides a number distribution. We calculated the proportion of that species within the entire spectrum by dividing the area of that species by the total area of all species present. Data presented in the Results and Discussion section refer to the proportion, that is, the mole fraction, of that particular species. A complete spectrum integration includes the full accessible spectral range from 150 to 2000 Da. Multiply charged species are not considered because they occur as singly charged species elsewhere in the spectrum and are accounted for then. The integration of only one single repeat unit leads to erroneous results as the species composition changes with polymer chain length. Such changes are caused by relative shifts in the various product distributions relative to each other and thus make the ratio determination at the repeat unit level meaningless.

A limitation of the above method is that a positive slope on the peak being integrated will yield an overestimation of the actual area; conversely, a negative slope will yield an underestimation of the actual area. This is an error inherent in the trapezoidal rule algorithm used to compute areas. Thus, all sample analysis proportions derived from integrals have been rounded to the nearest percent. Any attempt to increase the accuracy to finer detail is considered to be unwise. The mass spacing for data acquisition in the mass spectrometer is 0.0667 Da and corresponds to the variable $\Delta m/z$ in eq 1. This is of consequence only to point out that a larger spacing would result in larger errors; conversely, a smaller spacing would reduce these errors. Figure S1 in the Supporting Information presents an actual TCP peak in the sample prepared at 100 °C in the presence of 0.005 mol·L^{-1} 1-octanethiol. Appropriate labels have been inserted to indicate the values corresponding to variables in eq 1, and a and b are the limits of integration, which correspond to the end values that enclose the peak and its isotopic pattern. The dark gray area is one incremental area; many such small areas are summed to provide the area of this TCP peak.

To ensure that the derived concentration profiles are truly (or as close as possible to) quantitative, the issue of potential ionization bias effects must be addressed. Ionization suppression effects can lead to slightly biased peak proportions if the suppression of ionization occurs as a result of different end-group functionalities being present. In the context of a previous study on polyacrylates,[31] an investigation into the extent of ionization differences was carried out, where a mixture of 1-octanethiol mediated poly(BA) and a poly(BA) macromonomer of the exact same structure as one of the β-scission products[37] was prepared, and an ESI-MS spectrum was taken in which the relative abundance of peak proportions agreed with the initial mixing ratio. An absolute error in the determination of peak abundances (and hence product composition) of <20% is assumed. Other studies[28,29] have shown that ionization occurs on the polymer backbone, and thus end groups have relatively little effect on ionization ability. It can therefore be presumed with a high degree of confidence that ionization suppression does not prove to be a significant constraint or limitation in undertaking a quantitative analysis of the data presented herein.

Table 1. Theoretical and Experimental Masses of the Monoisotopic Peaks of Products Occurring in the Chain-Transfer Polymerization of BA with 1-Octanethiol in the m/z range of 1575−1703 Da in the Presence of Either AIBN (60−100 °C) or ACHN (120−140 °C) as an Initiator[a]

species	$m/z_{\text{theoretical}}$ (Da)	$m/z_{\text{experimental}}$ (Da)[b]	$\lvert\Delta m/z\rvert$
TCP	1578.02	1578.0	0.02
β^{I}	1687.97	1688.1	0.03
β^{II}	1590.02	1590.1	0.05
β^{III}	1676.10	1676.0	0.10
a	1594.03	1593.8	0.23
b	1541.00	1541.1	0.07
b′	1629.05	1629.0	0.05
$\beta^{\text{II}}{}_{\text{AIBN}}$	1641.14	1641.0	0.14

[a] All masses correspond to sodium adducts. [b] The given values refer to those that the data obtained for the sample made at 100 °C and an octylthiol concentration of 0.005 mol·L^{-1}, and in the case of the ACHN-specific product, to a sample prepared at 140 °C. Virtually identical m/z are found in all spectra.

Results and Discussion

All peaks present in the spectrum were assigned, and a detailed discussion of MCR behavior in the present system has been given before;[31] see Table 1 for masses and Schemes 1 and 2 for the structures associated with these masses.

All product species identified in the spectra can be found in Schemes 1 and 2. It must be noted that β-scission reactions produce four fragments, but one of these fragments is identical to the propagating chain SPR and thus cannot be distinguished as a fourth discrete product via ESI-MS. In intermolecular transfer, a terminally propagating radical abstracts a hydrogen atom from another polymer molecule, whereas in intramolecular transfer, a [1,5] H-shift reaction results in a hydrogen abstraction via a six-membered ring structure; in both cases, an MCR is formed, and in a chain-transfer-dominated system, they are of the same end-group composition. β-scission of the MCR then yields the three products denoted as $\beta^{\text{I–III}}$ and a radical fragment identical to the SPR. In Scheme 2, the thiol group (denoted by a T) could alternatively be an AIBN- or ACHN-initiating fragment. In this case, β-scission results in the formation of species $\beta^{\text{II}}{}_{\text{AIBN}}$ or $\beta^{\text{II}}{}_{\text{ACHN}}$. In addition, other reactions may occur, such as radical addition to the β^{I} and β^{II} species. Also, the radical scission product that leads to the formation of β^{III} may undergo its specific scission and transfer reactions. However, in all of these reactions, no structurally different species from the those shown are generated.

Figure 1 shows a typical mass spectrum obtained via ESI-MS of poly(BA) at high temperatures and a low amount of transfer agent. Without the effects of the transfer agent, the main species (β^{I}) is formed by β scission and comprises the vast majority of product seen, that is, 59% of the total product. β-scission products $\beta^{\text{I–III}}$ make up a total of 78%. It is not possible to determine how much of the SPR species originates from β scission because the number of chains that undergo backbiting and subsequently how many of those MCRs undergo β scission along the pathway that yields the SPR and β^{I} species cannot be determined. Furthermore, due to intramolecular transfer being an isobaric transformation, it is fundamentally not possible to determine how many backbiting steps one growing chain has already undergone in its lifetime.

Figure 2 shows a typical repeat unit of the sample shown in its entirety in Figure 1, whereas Figure 3 depicts an experiment

Scheme 1. Some Products Found in the Chain Transfer Polymerization of BA with 1-Octanethiol

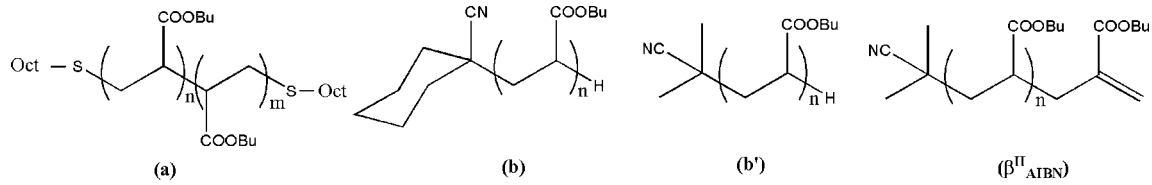

Scheme 2. Formation Pathways of *β*-Scission Products via the Midchain Radical Species in the Presence of 1-Octanethiol as Transfer Agent

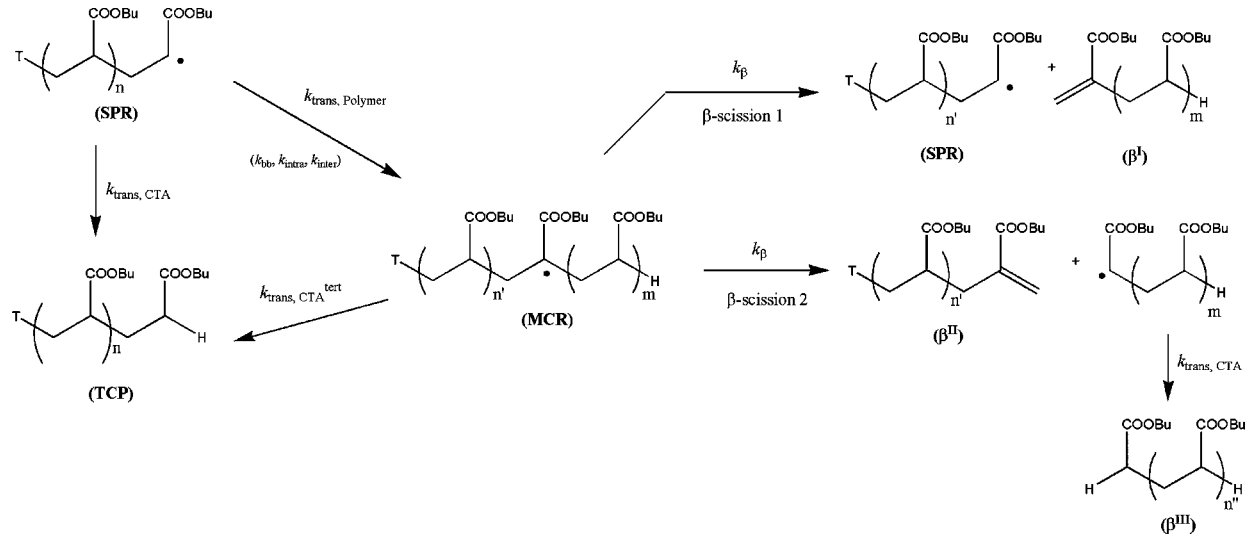

conducted under similar conditions with 0.4 mol·L^{-1} 1-octanethiol content rather than the much lower 0.005 mol·L^{-1} of Figure 2. An inspection of Figure 2 shows that the vast majority of total product is formed from *β*-scission. Smaller amounts of TCP and conventional combination product can also be seen. Because of the high molecular weight of this sample, multiply charged species are also present. Schemes 1 and 2 present the structures of these species. An inspection of Figure 3 reveals that the thiol-capped polymer, TCP, is the most abundant, whereas the *β*-scission products now contribute a markedly smaller proportion. It is noteworthy that the repeat unit depicted corresponds to a DP_n of 11 for species TCP and a, and a DP_n of 12 for all other species present.

By comparing Figures 2 and 3, it can be seen that at lower concentrations of 1-octanethiol, smaller amounts of TCP are identified in the mass spectrum. At low concentrations of thiol and relatively high temperatures (e.g., $c_{thiol} < 0.05$ mol·L^{-1} and $T > 80$ °C), *β*-scission reactions dominate transfer and

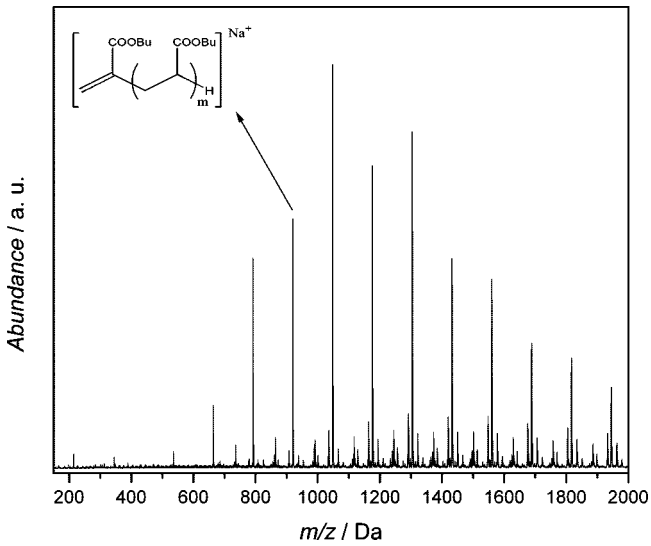

Figure 1. Typical ESI-MS spectrum of polymer obtained from bulk polymerization of butyl acrylate at 100 °C in the presence of 5×10^{-3} mol·L^{-1} 1-octanethiol initiated by 5×10^{-3} mol·L^{-1} AIBN. The polymerization was carried out for 20 min with AIBN as an initiator and had a conversion of 96%.

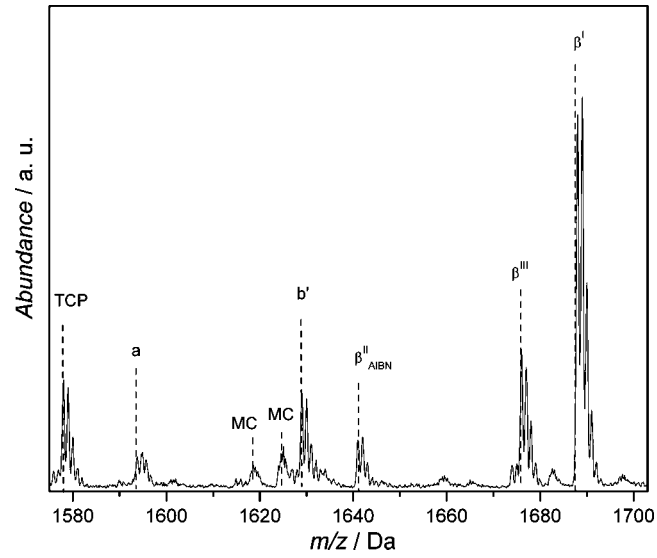

Figure 2. Typical ESI-MS spectra of polyBA obtained from bulk polymerization at 100 °C with 0.005 mol·L^{-1} 1-octanethiol. The polymerization was initiated by 5×10^{-3} mol·L^{-1} AIBN. This is a repeat unit in the range of 1575−1703 Da with assigned species. The dashed lines represent the $m/z_{theoretical}$, and MC denotes multiply charged peaks. Please refer to Schemes 1 and 2 for structures of the individual species.

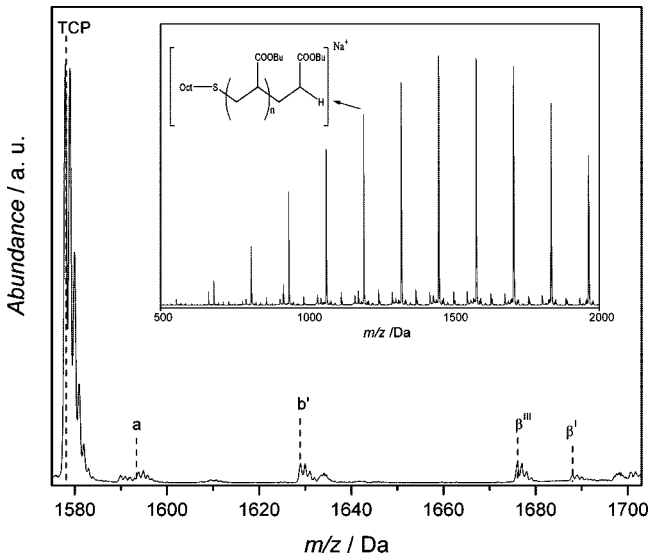

Figure 3. Typical ESI-MS spectra of polyBA obtained from bulk polymerization at 100 °C with 0.4 mol·L^{-1} 1-octanethiol. Polymerization was initiated by 5×10^{-3} mol·L^{-1} AIBN. This is a representative repeat unit in the range of 1575−1703 Da with assigned species. The insert shows the full spectrum with the main TCP product labeled. Please refer to Schemes 1 and 2 for structures of the individual species.

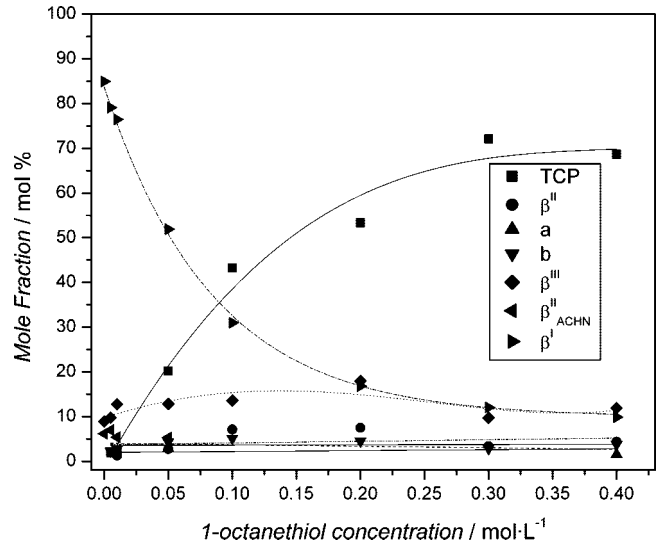

Figure 4. Change in mole fraction of individual polymer species from BA polymerizations in experiments conducted at 140 °C under varying concentrations of 1-octanethiol. Note that all lines are to guide the eye only and do not represent an actual fit. Please refer to Schemes 1 and 2 for structures of the individual species.

conventional termination. β-scission products constitute 78% of the whole product spectrum depicted in Figures 1 and 2. In Figure 3, where 0.4 mol·L^{-1} thiol was employed, the TCP product accounts for 81% of the product whereas the β-scission products are only 11%. This is a trend seen in all samples whereby higher concentrations of 1-octanethiol produce higher amounts of TCP in the final polymer. Generally, small amounts of termination via combination product a (structure in Scheme 1) are found in all samples.

All occurring product peaks in the CTA/BA system are unambiguously assigned. Figures 2 and 3 show only a particular repeat unit representing the samples. However, the relative amounts of species might (and indeed do) change with the DP_n. Thus, as is described in detail in the Data Analysis section, quantitative mole fractions of all species are deduced from integration over all repeat units. Figure 4 depicts a graph of the mole fraction of all species found versus the concentration of 1-octanethiol in samples prepared at 140 °C, which is the highest temperature studied herein because BA boils at 144 °C at ambient pressure. This temperature was also chosen because β scission is known to occur predominantly under those conditions and is thus the best way to assess the effect of adding 1-octanethiol on product constituents, as we demonstrated in our last publication.[31] From Figure 4, the variation of the proportion, and hence mole fraction, of the different species as the concentration of 1-octanethiol is changed can be seen. Such a graph emphasizes trends and highlights the species that are most sensitive to increasing thiol concentration. The Figure undoubtedly reveals that at high temperatures, TCP and β^I show the largest variation in mole fraction and are thus the main products of interest with respect to the thiol concentration variation. In addition, it is clear that all other species do not show significant variation with increasing thiol concentration. The formation of species β^I is very sensitive to the thiol concentration. Increasing the thiol concentration from 0.01 to 0.05 mol·L^{-1} results in the TCP proportions increasing from 2 to 20% and the β^I proportions decreasing from 76 to 52%. At a concentration of 0.4 mol·L^{-1}, β^I becomes a minor product, constituting 10% of the product spectrum. The decrease in TCP with decreasing thiol concentration is an obvious effect of having less chain transfer activity during polymerization. Concomitantly, the relative amounts of the β^I species increase because β-scission is, as mentioned above, predominant in the absence of transfer. In principle, similar amounts of the individual β-scission products are expected because the scission is not favored to occur to either side of the MCR. The fact that much higher concentrations of β^I are found (i.e., the unsaturated polymer carrying only a proton end group on the saturated chain end) may be explained by a complex set of equilibria between the scission products and the MCRs because β-scission is in principle a reversible reaction. As was demonstrated in a recent study, such equilibria favor the formation of β^I because of the additional driving force of the backbiting reaction.[37] In fact, in the high-temperature initiator-free solution polymerization of BA, where polymerization occurs under conditions of a very low radical flux, only β^I can be found in the product. This observation fits to the experimental finding of almost equal amounts of all scission products in the case of high thiol content because the patching of the MCR via proton transfer from the thiol interrupts such equilibria. At lower thiol concentrations, disparate amounts of β^I to β^{II} and β^{III} are identified under all conditions investigated.

It addition, it needs to be emphasized that transfer to polymer onto a remote backbone site (in other words, not via a six-membered ring structure) plays a major role because β^I with comparatively high DP_n is seen. If transfer mostly occurs via a six-membered ring, then β^I with a chain length of only three is expected. Such species may be present but could not be found in larger quantities, which suggests that at least at high monomer conversion, other transfer to polymer pathways (i.e., inter- and intramolecular transfer to remote backbone locations)[13] is as important as the backbiting reaction that is dominant in low-conversion systems. This finding is in good agreement with studies that were carried out in the context of RAFT−star polymerization, where star−star coupling upon intermolecular transfer is clearly observable.[26,38]

Trends for minor species are difficult to ascertain; therefore, the following discussion on changing reaction temperature will focus on the species β^I and TCP because they show the largest variation in relative product concentration. At this point, it should be stressed that a large data basis was obtained for this study. Polymer samples for a large number of different reaction

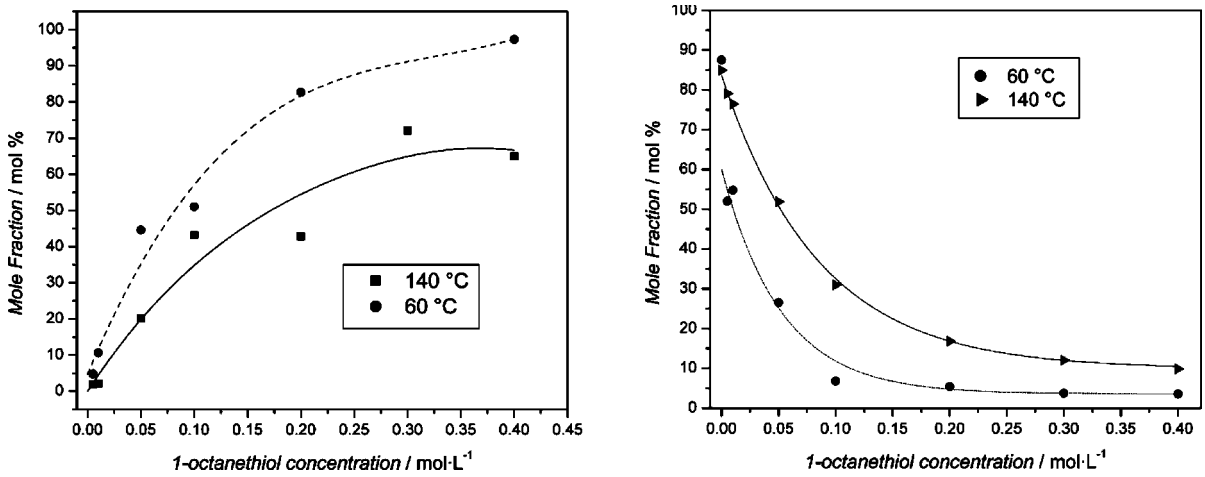

Figure 5. Mole fraction of TCP product formed at various concentrations of 1-octanethiol at 140 and at 60 °C (left) and mole fraction of β^{I} under the same conditions (right). At 60 °C, AIBN was used as an initiator, whereas at 140 °C, ACHN was used. Note that all lines are to guide the eye only and do not represent an actual fit. TCP and β^{I} structures can be seen in Schemes 1 and 2.

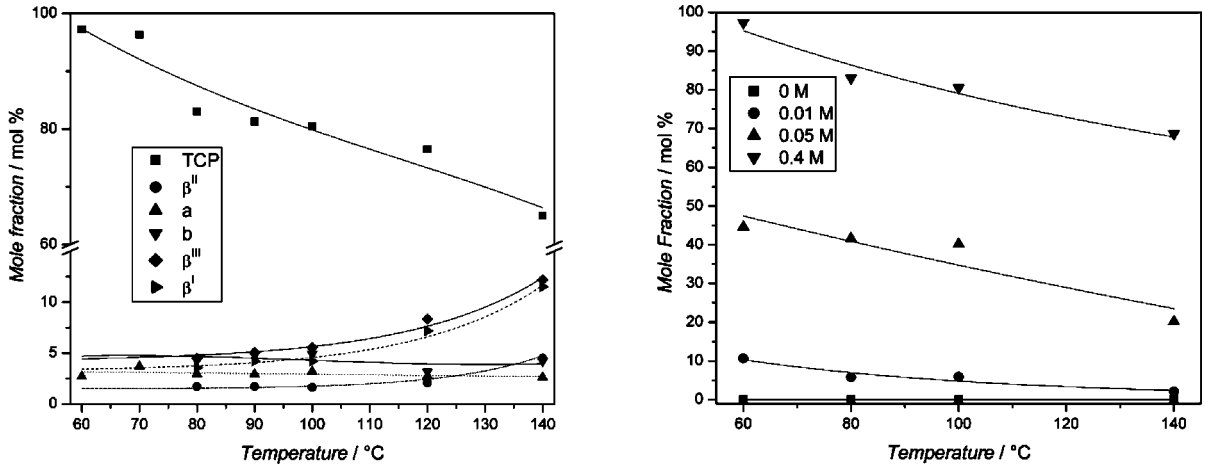

Figure 6. Variation in the proportion of species present over a range of temperature when all samples contain 0.4 mol·L^{-1} 1-octanethiol (left). Proportions of the main TCP product at varying temperature and varying concentration of 1-octanethiol (right). Note that all lines are to guide the eye only and do not represent an actual fit. Furthermore, note the break in the vertical axis (left). All chemical structures of species present can be seen in Schemes 1 and 2.

conditions were obtained and subjected to MS analysis. For the sake of clarity, not all data are displayed and discussed in full detail. However, all important kinetic effects are explained on selected representative data sets, whereas the full data are tabulated in the Supporting Information in Tables S1−S5. Figure 5a shows how the mole fraction of TCP product changes when increasing amounts of 1-octanethiol are added to the reaction mixture at different temperatures. As more thiol is added, more TCP product is found in the final polymer because the thiol is a highly effective chain transfer agent (CTA). Furthermore, it can be seen that at 140 °C, less TCP is found when compared with the respective samples containing the same concentrations of thiol at 60 °C. Figure 5b shows the mole fractions of the most abundant β-scission species β^{I} at 60 and 140 °C. Accordingly, less scission products are found at high thiol content at lower temperatures. About 10% of the final product consists of β^{I} at the highest thiol concentration at 140 °C, whereas almost none can be found at 60 °C. Because β-scission reactions are predominant at higher temperatures, such an observation comes as no surprise and shows that the CTA cannot prevent all side reactions from occurring at higher temperatures even though proton transfer onto the MCRs is still highly effective, as is pointed out above. As can be expected because of backbiting and β-scission, significantly more β^{I} product is formed at 140 °C (85%) compared with the respective samples at 60 °C (56%). In addition, it can be observed that as thiol concentration increases, an almost exponential decrease is seen in the amount of β^{I}. TCP is the main species seen at thiol concentrations of >0.05 mol·L^{-1}, irrespective of the temperature at which the sample was prepared; however its mole fraction increases with increasing thiol concentration. This is most evident when looking at the TCP peaks in Figures 2 and 3. Conversely, β^{I} is the main product seen at all thiol concentrations of <0.05 mol·L^{-1}, irrespective of the preparation temperature. In this case, the mole fraction of β^{I} increases with decreasing thiol concentration, which proves that β-scission plays an important role, even at moderate polymerization temperatures.

Lastly, it is of interest to examine the effect of temperature on the formation of various species. It must be noted that two initiators were used because no suitable initiator with a reasonable half life for conducting experiments in the range of 60−140 °C is available. For this reason, AIBN was used as the initiator for all experiments up to and including 100 °C. Above 100 °C, ACHN was used. Figure 6a presents data illustrating the change in product composition with temperature at a fixed thiol concentration of 0.4 mol·L^{-1}. The break in the vertical axis of Figure 6a takes into account the fact that the apparently large increase in β^{I} and β^{III} is still comparatively small when compared with changes in the TCP product. The proportion of

TCP decreases from 97 to 67% as the temperature is increased. Such a shift with temperature is caused by increasing β-scission reactions, as was already identified in the context of Figure 5. In the present case, the minor products β^{I} and β^{III} are seen to double as the temperature is increased from 100 to 140 °C because of the overall increased importance of β scission at higher temperatures. A closer inspection of Figure 6a shows that there is 2−5% more β^{I} than β^{II} according to the general dominance of β^{I} (see above). Figure 6b shows the proportions of the main TCP product from 60 to 140 °C at four incremental concentrations of 1-octanethiol, varying from 0 to 0.4 mol·L^{-1}. It is clear that irrespective of thiol concentration the proportion of TCP product decreases as the temperature increases. This trend is again readily explained as increasing amounts of β-scission products are formed with increasing temperature. At 0 mol·L^{-1} concentration of thiol, obviously no TCP product is found.

Survey of Data and Consideration of Less-Abundant Side Products. CTA and temperature are counteracting forces when it comes to controlling the amounts of side products formed via β-scission. On one hand, increasing the reaction temperature creates a greater variety of different types of species and increases the amount of β-scission products formed; on the other hand, increasing the concentration of 1-octanethiol added to reaction mixtures leads to increasing amounts of TCP product formation and suppresses the formation of β-scission products (known as the patcher effect in our previous publication).[31] The products that have been found are TCP (if thiol is present), conventional termination products a, b, or b′, and β-scission products β^{I}, β^{II}, and β^{III} as well as β^{II}_{AIBN} or β^{II}_{ACHN}. The composition of a particular polymer sample depends on a combination of the effects of thiol concentration and reaction temperature. The two parameters determine which products are found and in what amounts. However, information regarding general trends can be deduced from the samples prepared under the extremes of the selected conditions. At low temperature and high concentration of thiol (i.e., the sample prepared at 60 °C with the addition of 0.4 mol·L^{-1} 1-octanethiol), 97% of polymer formed is the TCP species with the remaining 3% being species a. At high temperature (140 °C) and high concentration of thiol (0.4 mol·L^{-1}), only 69% of the total product spectrum is TCP product. Species a (1%), b (4%), β^{I} (10%), β^{II} (4%), and β^{III} (12%) are also found and constitute the remaining proportions in the sample. At 0.005 mol·L^{-1} thiol concentration at 140 °C, TCP is a mere 2% of the total, with β^{I} being the major product at 79% and β^{II}_{ACHN} (7%) with β^{III} (10%) and b (2%) being the remaining constituents. The last extreme is at low thiol concentration (0.005 mol·L^{-1}) and low temperature (60 °C). This sample had 5% TCP, 4% a, 13% b′, 7% β^{II}_{AIBN}, 18% β^{III}, and 53% β^{I}. Samples with 0 mol·L^{-1} thiol do not contain any TCP product, rather they contain amounts of b′ (17%), β^{II}_{AIBN} (12%), β^{III} (15%), and β^{I} (56%) in the case of low temperature (i.e., 60 °C) and β^{II}_{ACHN} (6%), β^{III} (9%), and β^{I} (85%) at high temperature (i.e., 140 °C).

Conclusions

An in-depth study of the product spectrum formed in the bulk polymerization of BA was conducted to examine the effects of elevated temperatures and varying concentrations of 1-octanethiol as a CTA. ESI-MS allowed detailed mapping of the product spectrum in acrylate polymerization to be carried out, and a novel evaluation method was proposed for data treatment and evaluation of the polymer formed. Clear trends for all species with variation of temperature and thiol concentration were identified, proving the robustness of the employed integration method. The main product peak found in the ESI-MS spectra obtained from polymer made by 1-octanethiol mediated polymerization at higher thiol concentrations was the expected transfer to thiol product, TCP, with small amounts of termination products also being present. At lower thiol concentrations, mainly β-scission products were found, even at a moderate reaction temperature of 60 °C. At all thiol concentrations, the expected β-scission products could be identified with β^{I} being the most abundant product by far under all conditions. This disparity is explained by equilibration of the scission products with the MCRs. At elevated temperatures, β-scission products are generally more prevalent, and between the extremes (from 60 to 140 °C and 0 to 0.4 mol·L^{-1} CTA) a comprehensive exploration of the product spectra was conducted, providing detailed quantitative data on the influence of temperature and the presence of varying amounts of CTA 1-octanethiol in BA polymerization.

Acknowledgment. C.B.-K. acknowledges funding from the Karlsruhe Institute of Technology (KIT) within the framework of the German Excellence Initiative for leading German universities as well as the German Research Council (DFG). S.P.S.K is grateful for the past receipt of an Australian Post Graduate Award. For the work carried out at CAMD, we thank Dr. Leonie Barner and Istvan Jacenyik for their excellent management of CAMD.

Supporting Information Available: Details of the integration procedure and individual integration results for all species. This material is available free of charge via the Internet at http://pubs.acs.org.

References and Notes

(1) Theis, A.; Feldermann, A.; Charton, N.; Davis, T. P.; Stenzel, M. H.; Barner-Kowollik, C. *Polymer* **2005**, *46*, 6797–6809.
(2) Nikitin, A. N.; Hutchinson, R. A. *Macromolecules* **2005**, *38*, 1581–1590.
(3) Junkers, T.; Theis, A.; Buback, M.; Davis, T. P.; Stenzel, M. H.; Vana, P.; Barner-Kowollik, C. *Macromolecules* **2005**, *38*, 9497–9508.
(4) Asua, J. M.; Beuermann, S.; Buback, M.; Castignolles, P.; Charleux, B.; Gilbert, R. G.; Hutchinson, R. A.; Leiza, J. R.; Nikitin, A. N.; Vairon, J. P.; van Herk, A. M. *Macromol. Chem. Phys.* **2004**, *205*, 2151–2160.
(5) Ahmad, N. M.; Heatley, F.; Lovell, P. A. *Macromolecules* **1998**, *31*, 2822–2827.
(6) Chiefari, J.; Jeffery, J.; Mayadunne, R. T. A.; Moad, G.; Rizzardo, E.; Thang, S. H. *Macromolecules* **1999**, *32*, 7700–7702.
(7) Plessis, C.; Arzamendi, G.; Alberdi, J. M.; van Herk, A. M.; Leiza, J. R.; Asua, J. M. *Macromol. Rapid Commun.* **2003**, *24*, 173–177.
(8) Arzamendi, G.; Plessis, C.; Leiza, J. R.; Asua, J. M. *Macromol. Theory Simul.* **2003**, *12*, 315–324.
(9) Willemse, R. X. E.; van Herk, A. M.; Panchenko, E.; Junkers, T.; Buback, M. *Macromolecules* **2005**, *38*, 5098–5103.
(10) Buback, M.; Hesse, P.; Junkers, T.; Sergeeva, T.; Theis, T. *Macromolecules* **2008**, *41*, 288–291.
(11) Busch, M.; Müller, M. *Macromol. Symp.* **2004**, *206*, 399–418.
(12) Peck, A. N. F.; Hutchinson, R. A. *Macromolecules* **2004**, *37*, 5944–5951.
(13) Junkers, T.; Barner-Kowollik, C. *J. Polym. Sci., Part A: Polym. Chem.* **2008**, *46*, 7585–7605.
(14) Nikitin, A. N.; Hutchinson, R. A.; Buback, M.; Hesse, P. *Macromolecules* **2007**, *40*, 8631–8641.
(15) Barner-Kowollik, C.; Davis, T. P.; Stenzel, M. H. *Polymer* **2004**, *45*, 7791–7805.
(16) Szablan, Z.; Lovestead, T. M.; Davis, T. P.; Stenzel, M. H.; Barner-Kowollik, C. *Macromolecules* **2007**, *40*, 26–39.
(17) Szablan, Z.; Junkers, T.; Koo, S. P. S.; Lovestead, T. M.; Stenzel, M. H.; Davis, T. P.; Barner-Kowollik, C. *Macromolecules* **2007**, *40*, 6820–6833.
(18) Lovestead, T.; Hart-Smith, G.; Davis, T. P.; Stenzel, M. H.; Barner-Kowollik, C. *Macromolecules* **2007**, *40*, 4142–4153.
(19) Hanton, S. D. *Chem. Rev.* **2001**, *101*, 527–569.
(20) Prokai, L. *Int. J. Polym. Anal. Charact.* **2001**, *6*, 379–391.
(21) Montaudo, G. *Trends Polym. Sci.* **1996**, *4*, 81–86.
(22) Scrivens, J. H.; Anthony, A. T. *Int. J. Mass Spectrom.* **2000**, *200*, 261–276.
(23) McEwen, C. N.; Peacock, P. M. *Anal. Chem.* **2002**, *74*, 2743–2748.
(24) Peacock, P. M.; McEwen, C. N. *Anal. Chem.* **2004**, *76*, 3417–3427.

(25) Peacock, P. M.; McEwen, C. N. *Anal. Chem.* **2006**, *78*, 3957–3964.
(26) Hart-Smith, G.; Chaffey-Millar, H.; Barner-Kowollik, C. *Macromolecules* **2008**, *41*, 3023–3041.
(27) Chaffey-Millar, H.; Hart-Smith, G.; Barner-Kowollik, C. *J. Polym. Sci., Part A: Polym. Chem.* **2008**, *46*, 1873–1892.
(28) Buback, M.; Frauendorf, H.; Vana, P. *J. Polym. Sci., Part A: Polym. Chem.* **2007**, *42*, 4266–4275.
(29) Buback, M.; Frauendorf, H.; Günzler, F.; Vana, P. *Polymer* **2007**, *48*, 5590–5598.
(30) Buback, M.; Frauendorf, H.; Günzler, F.; Vana, P. *J. Polym. Sci., Part A: Polym. Chem.* **2007**, *45*, 2453–2467.
(31) Junkers, T.; Koo, S. P. S.; Davis, T. P.; Stenzel, M. H.; Barner-Kowollik, C. *Macromolecules* **2007**, *40*, 8906–8912.
(32) Grady, M. C.; Simonsick, W. J.; Hutchinson, R. A. *Macromol. Symp.* **2002**, *182*, 149–168.
(33) Quan, C.; Soroush, M.; Grady, M. C.; Hansen, J. E.; Simonsick, W. J. *Macromolecules* **2005**, *38*, 7619–7628.
(34) Feldermann, A.; Coote, M. L.; Stenzel, M. H.; Davis, T. P.; Barner-Kowollik, C. *J. Am. Chem. Soc.* **2004**, *128*, 5915–15923.
(35) Penzel, E.; Götz, N. *Angew. Makromol. Chem.* **1990**, *178*, 191–200.
(36) Strazielle, C.; Benoit, H.; Vogl, O. *Eur. Polym. J.* **1978**, *14*, 331–334.
(37) Junkers, T.; Bennet, F.; Koo, S. P. S.; Barner-Kowollik, C. *J. Polym. Sci., Part A: Polym. Chem.* **2008**, *46*, 3433–3437.
(38) Boschmann, D.; Vana, P. *Macromolecules* **2007**, *40*, 2683–2693.

MA801196W